Du *et al. Herit Sci (2021) 9:103*
https://doi.org/10.1186/s40494-021-00582-5

Heritage Science

RESEARCH ARTICLE

Open Access

Study on the linear absent section ratio (L-ASR) of earthen sites and anthropogenic influence from the perspective of population density

Yumin Du[1,2*], Wenwu Chen[3], Kai Cui[4], Wenqiang Dong[1,2], Shuai Zhang[3] and Qiyong Zhang[3]

Abstract

Having extremely high artistic, scientific and social values, earthen sites are widely distributed in China and are important human cultural relic resources. Due to accumulated natural erosions (from rain and wind) and human activities (destructive activities of human beings in history and modern times), however, earthen sites have been greatly damaged, and many sections have even been absent, so that they are seriously threatened by extinction. Under these circumstances, acquiring the conservation status of earthen sites is a vital prerequisite for the subsequent targeted protection. In this paper, as a world-renowned heritage site, the castles of the Ming Great Wall located in Qinghai Province were selected as the research object. A novel indicator, namely the linear absent section ratio (L-ASR), was proposed, and its value was classified into five levels to quantitatively characterize the specific conservation status of such sites, including excellent (E) (0–10%), good (G) (10–25%), fair (F) (25–50%), poor (P) (50–75%), and very poor (VP) (75–100%). Based on the assessment results, the castles with excellent status constituted the minimum proportion, while the castles with very poor status represented the largest percentage, reflecting the grave situation of earthen sites. Furthermore, by applying population distribution models to the linear fitting combined with the population density (PD), a positive correlation between PD and L-ASR was obtained to reveal the anthropogenic influence on the destruction of earthen sites. Principal component analysis (PCA) was utilized to provide a far richer understanding of which factors correlate most strongly with deterioration. This study provides a new thought to quantitatively characterize the preservation conditions of earthen sites and also indicates the effect of human activities on the damage of earthen sites from a population density perspective, which is potentially used for the analysis of more various types of architecture with different construction techniques. Hence, this approach is beneficial to the overall damage assessment of earthen sites, and also meaningful to their further preservation and protective planning.

Keywords: Earthen sites, Ming Great Wall, Population density, Anthropogenic influence

Introduction

Earthen sites are typical architectural sites mainly built with soil materials, and they are widely distributed throughout the world in places such as Ajina Tepa, Tajikistan [1], Alhambra, Spain [2], the Casa Grande Ruins National Monument, the United States [3], Çatalhöyük, Turkey [4], and the Great Wall [5] and Tulou, China [6]. The earth was also specifically used for military architecture located in Southern Europe and North Africa, such as the defense wall with rifle ports in Spain, the fortresses in Portugal, and Muslim fortifications in North Africa [7–9]. Having extremely high artistic, scientific and social values, earthen sites in China have a

*Correspondence: duym@nwpu.edu.cn
[1] Institute of Culture and Heritage, Northwestern Polytechnical University, Xi'an 710072, China
Full list of author information is available at the end of the article

long historical process stretching from the Paleolithic Age to modern times, reflecting the evolution of Chinese civilization and the improvement of social productivity [10, 11]. There are many earthen sites located in NW China, and the climatic location of these sites has harsh weather characteristics, including drought, low rainfall, high winds and strong evaporation. Undoubtedly, they are important human cultural relic resources. Because of exposure to long-term natural forces, including wind and rain erosions and human activities, these earthen sites have developed many deteriorations, such as sapping, cracks, scaling off, gullies, collapses, etc., severely threatening their preservation [5, 12–15]. Under the current circumstances, most earthen sites have been seriously damaged, and many sections have even been absent due to the development of deteriorations and natural/human influences over thousands of years, so their existence is greatly threatened. Consequently, the targeted protection of earthen sites is very urgent, and securing the conservation status of these earthen sites starting from these absent sections is a vital prerequisite for the protection work.

To date, many scholars have mainly focused on the mechanisms of deterioration at earthen sites, as listed in Table 1: Four deterioration categories, including property deterioration, structure damaging, structure collapse, and site destroying, have been identified [13]; On the basis of field investigation and laboratory analysis, four main deterioration modes, namely wind-related deterioration, water-related deterioration, temperature-related deterioration and chemical-related deterioration were identified at the Jiaohe ruins in China [15]; A model characterizing the deterioration at the earthen sites of the Ming Great Wall in Qinghai Province was also proposed to reveal the mechanisms and evolution of deterioration from a macro perspective [5]. Based on these deterioration developments, the damage assessment of earthen sites was studied by means of multicriteria decision-making (MDCM) and machine learning methods combined with environmental factors and building material indices, which revealed the local damage to earthen sites caused by the development of deteriorations [12, 16]. However, a scientific approach to assess the overall damage of earthen sites and quantitatively illustrate their conservation status is still lacking. The effects of natural factors on earthen sites, such as wind, rain, earthquakes, etc., have mostly been studied [14, 17, 18], but few studies have focused on the quantitative influence of human activities.

In fact, human activities have very significant effects on the damage of earthen sites, and even artificial destruction in historical and contemporary processes has been regarded as a deterioration type [11, 13, 15]. For instance, local farmers directly dug soils at earthen sites (Fig. 1a), randomly add buildings along with earthen sites (Fig. 1b), and even dwell behind earthen sites so that the earthen wall is used as a home enclosure (Fig. 1c and d). Some farming activities (Fig. 1e) and road engineering (Fig. 1f) activities have also influenced earthen sites conservation. However, to implement the Rules on the Great Wall Protection, the overall protective planning of the Ming Great Wall in Qinghai Province has been conducted in an orderly manner, which has effectively restricted human destruction under the joint governmental and individual efforts [19]. To protect the Ming Great Wall in Qinghai Province, conservation management and protection systems have been established and improved. Specifically, the local protection departments have set up logs and files for the Great Wall sections for which they are responsible, the government has strengthened related law enforcement, scholars are using advanced technology and materials to consolidate damaged earthen sites, and regulators have combined the technical monitoring and manual monitoring approaches to prevent human activities. Such work has effectively slowed down the destruction process of the Ming Great Wall. According to the research about the correlation between human activity intensity and population density by counties in China in 2008, there exists a positive exponential function with a high correlation coefficient ($R = 0.8156$) [20]. This means that the population density can be regarded as an effective

Table 1 The research status of the mechanisms of deterioration of earthen sites

Deterioration Types	Deterioration Causes	References
Property deterioration, structure damaging, structure collapse, and site destroying	Low precipitation with occasional very short heavy rainstorms, high temperature difference, high evaporation, freeze–thaw cycle, strong winds, and seismicity	[13]
Wind-related deterioration, water-related deterioration, temperature-related deterioration and chemical-related deterioration	Engineering properties of soil, stability of platform, and environmental impacts	[15]
Cracks, gullies, collapses, sapping, and scaling off	Engineering-related parameters of the rammed earth, meteorological factors, and building technologies	[5]

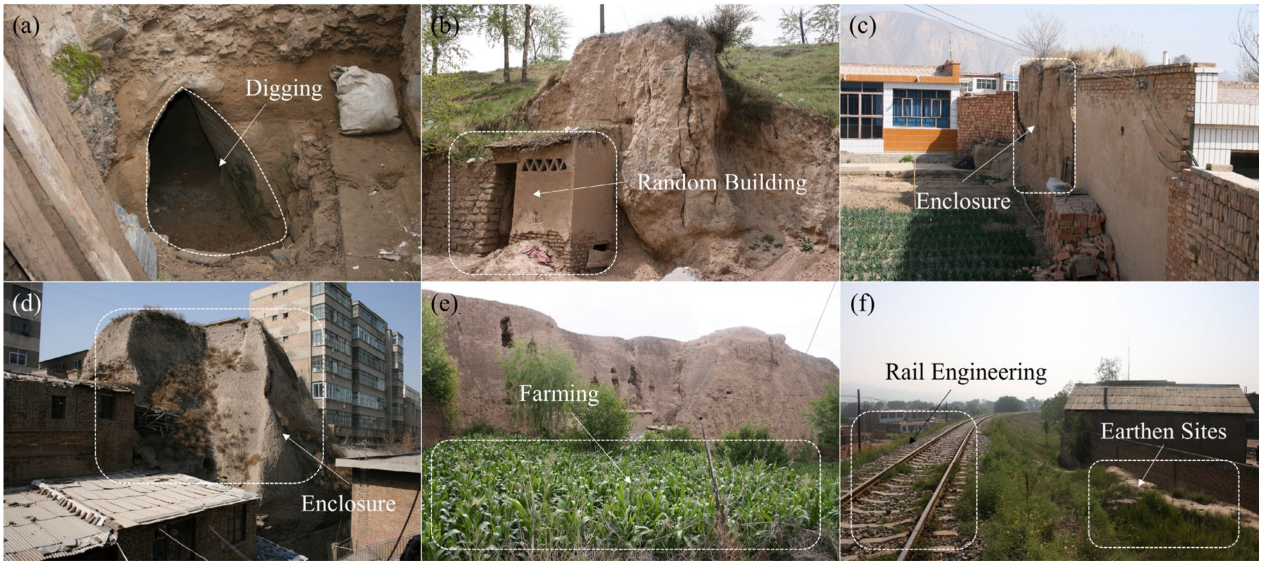

Fig. 1 The human activities graphs: a digging, b random building, c an enclosure in a peasant household, d an enclosure in an urban housing estate, e farming activities, and f rail engineering

indicator to show the degree of human activity, so it is a good metric to be used for assessing anthropogenic impact. Therefore, this research aims to investigate the anthropogenic influence on earthen sites from the perspective of population density.

In this paper, the authors selected 46 castles of the Ming Great Wall located in Qinghai Province, China, as the research object and proposed a novel indicator, namely the linear absent section ratio (L-ASR), to characterize the conservation of such sites. Moreover, as human destruction has been regarded as one of the typical deterioration types of earthen sites [13, 15], the authors decided to focus on the impact of humans as a correlation to earthen site damage in order to prove and determine their influence on earthen site damage. The anthropogenic influence on the L-ASR was researched from the perspective of population density (PD). By applying population distribution models, PD was further correlated with L-ASR to show the effect of human activities on the damage of earthen sites from a macroscopic perspective. The research results show the potential to promote the indicator and model proposed in this study into earthen sites and even many types of architecture built with any type of construction technique, because the materials and techniques of buildings were not considered in the assessment process proposed in this research. The research findings provide beneficial references to the overall damage assessment of earthen sites and are also meaningful to their further preservation and protective planning.

Study sites

The Great Wall built during the Ming Dynasty, called the Ming Great Wall, was the most renowned military defensive project in ancient China and was designated as a World Heritage in 1987 [21]. The Ming Great Wall is a complex military network consisting of walls, trenches, beacon towers, passes, castles, precipitous mountain areas, marine insurance, etc., and these building types played their respective roles and were coordinated for military defense [22]. In the whole Great Wall system, the castle was a core element with multiple functions, including the exchange of military information, goods and people, and the management of important civil affairs [23, 24].

Located independently from the Great Wall mainline in "nine towns", the Ming Great Wall in Qinghai Province is a significant section of the whole Great Wall, which was built from 1546 to 1596, surrounding Xining Wei with an arch shape [22, 25]. Due to the rammed earth being vulnerable to climate erosion, the Ming Great Wall has severely deteriorated as a form of earthen sites [16, 26]. As a significant part of the Ming Great Wall, 46 castles are located in Qinghai Province (Fig. 2), which were selected as the study object to research their conservation status. These castles coincide with the selection of case studies in a previous study on their architectural features and military functions [24], which is a significant extension and justification of our previous research. Information on these sites is listed in Table 2. As for the distribution of the 46 castles, some castles were located near the main wall, while some were located far away

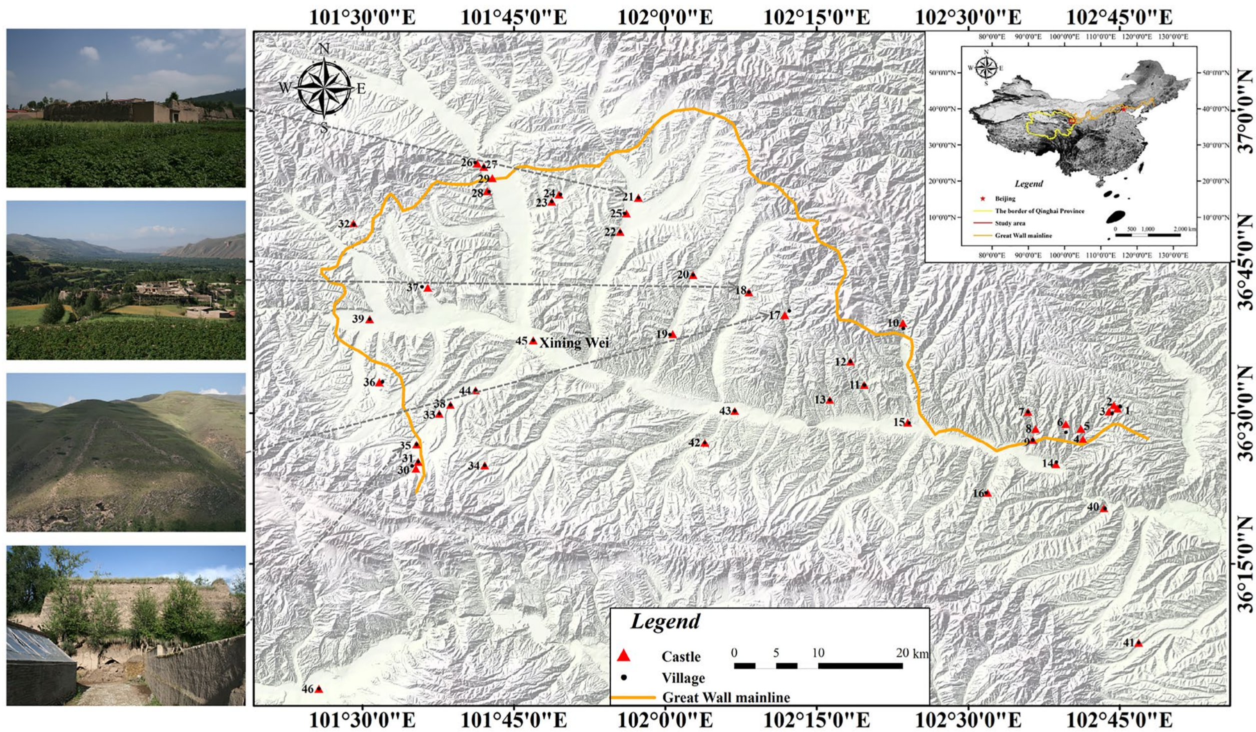

Fig. 2 The distribution of castles of the Ming Great Wall in Qinghai Province; the photos of the No. 17, No. 18, No. 21, and No. 35 castles have been studied in previous research [24]

from the mainline. The castle locations were closely related to their specific military functions: The farther the Great Wall mainline, the larger the castles were, and the more complex the military functions of the castles [24].

Methods

The Great Wall is one of the most representative lineal cultural heritage sites in China and has a linear distribution pattern across 15 Chinese provinces with a total length of 8851.8 km [27, 28]. To date, a large number of wall sections have been absent over the course of hundreds of years. It is important to measure the absent length of the wall when evaluating the conservation status of the Great Wall. In this research, the linear circumference indicates the whole length of the perimeter of the castles including their north, east, south and west walls, called circumference length (CL), and the length of remaining wall sections is called the remaining length (RL). Linear circumference data were collected from archaeological materials, including survey reports on the Ming Great Wall in Qinghai Province and castle plane graphs provided by the Qinghai Provincial Administration of Cultural Relics and the Qinghai Bureau of Surveying and Mapping, which organized comprehensive investigations on the Great Wall from 2007 to 2009. The wall length of castles can be extracted and measured from these materials.

By collecting archaeological materials from these such sites, the CL and RL of the walls can be acquired. According to the survey reports on the Ming Great Wall in Qinghai Province provided by the Qinghai Provincial Administration of Cultural Relics and the Qinghai Bureau of Surveying and Mapping, the length of remaining and absent wall sections can be collected. To correct this length data, the castle plane graphs provided by the Qinghai Provincial Administration of Cultural Relics and the Qinghai Bureau of Surveying and Mapping were imported in Auto CAD to measure the absent wall sections. The plane graphs were drawn by the archaeological investigation team using orientations and plotting scales to reflect the site plane layout.

The authors proposed a novel indicator called the linear absent section ratio (L-ASR), which is mainly applied to quantitatively characterize the ratio of the absent wall's linear length to the circumference length of the castles by measuring the CL and RL to reflect the overall damage or material damage of the lineal cultural heritage since they were built up, according to the following calculation:

$$\mathrm{L-ASR} = 1 - (\mathrm{RL}/\mathrm{CL}) \tag{1}$$

where RL/CL is the remaining length ratio (RLR). The castle CL and RL data can be acquired from the

Table 2 The information on castles of the Ming Great Wall in Qinghai Province

Castle number	Name	Castle number	Name
1	No.1 of Chengbeihou Castle	24	Xiamaquan Castle
2	No.2 of Chengbeihou Castle	25	Weiyuan Castle
3	Najiazhuang Castle	26	Miaogou Castle
4	Mengjiawan Castle	27	Xin Castle
5	Nianmugou Castle	28	Pingle Castle
6	Nianxiangou Castle	29	Gu Castle
7	Naozhuang Castle	30	Yangpotai Castle
8	No.1 of Simozhuang Castle	31	Shangxinzhuang Castle
9	No.2 of Simozhuang Castle	32	Boshiying Castle
10	Shangyamen Castle	33	Laoyou Castle
11	Lianxing Castle	34	Jiaerzang Castle
12	Qijia Castle	35	Xincheng Castle
13	Dieergou Castle	36	Yuanshaner Castle
14	Laoya Ancient Castle	37	Dongjiawan Castle
15	Nianbo Ancient Castle	38	Xujiazhai Castle
16	Yuanjiazhuang Castle	39	Tonghai Castle
17	Maying Castle	40	Songshu Castle
18	Beizhuang Ancient Castle	41	Gushan Ancient Castle
19	Shijia Castle	42	Baishen Castle
20	Xintian Castle	43	Zhongcun Castle
21	Baiya Castle	44	Zongzhai Castle
22	Datongyuan Castle	45	Xining Wei
23	Chenjiatai Castle	46	Guide Ancient Castle

measurement of plane graphs in Auto CAD. The proposed assessment methods are applicable to pre-existing architecture with other types of materiality because the index of L-ASR reflects the percentage of material mass that the element has lost, based on a comparison of surfaces measured in plane graphs.

The value of L-ASR can be classified into 5 levels to quantitatively characterize the specific conservation status of the castles, including excellent (E) (0–10%), good (G) (10–25%), fair (F) (25–50%), poor (P) (50–75%), and very poor (VP) (75–100%). Because there has not been a uniform method of damage division for earthen sites thus far, in this research, the authors mainly referred to the classification approach used for the rock quality designation (RQD), which is still the only rock mass classification index available. RQD is an index of rock quality in which a modified core recovery percentage is obtained by counting only pieces of sound core 10 cm or greater in the length of NX size or large core diameters, which is an important indicator of rock quality classification [29].

After that, the authors introduced the index of population density (PD) into this research. The PD indicates the number of people living in each unit of area (such as a square kilometer), which is an important indicator for measuring the distribution of population in a region [30]. Its formula was shown in Eq. (2):

$$PD = PN/RA \tag{2}$$

where PN is the number of population in a certain region, and RA is the area of that region. The population number of each village was collected from the survey results on the Ming Great Wall in Qinghai Province provided by the Qinghai Provincial Administration of Cultural Relics and the Qinghai Bureau of Surveying and Mapping, which organized comprehensive investigations on the Great Wall from 2007 to 2009. From that investigation activity, the population number in villages where castles were located in or nearby can be found in 2008. The population region of each village can be found and measured using Rivermap X3 software. By using the measuring tools in this software, the area of the population region can be determined.

Using the above procedures and methods, the L-ASR values of 46 castles can be acquired. The data of RL and CL can be collected, and then L-ASR data can be calculated based on Eq. (1), and the conservation status can be determined according to the L-ASR values and classification levels.

Finally, four frequently used single core population distribution models were applied to achieve positive correlations between PD and L-ASR, showing the influence of human activities on the conservation of earthen sites from a macroscopic perspective. Because the population number in this research is only collected from the archaeological materials in 2008 provided by the Qinghai Bureau of Cultural Heritage, and the L-ASR data can also reflect the destruction status of castles in 2008, as the overall survey of castles was carried out in that year, a good corresponding relationship between PD and L-ASR was determined in this paper. Some castles are located in villages, while others are located out of the villages at a certain distance. The distance should be a nonnegligible factor for the damage caused by human activities. The reason why four different core population models were used is that the distance between castles and villages can be considered as an important factor in the quantitative study of the anthropologic influence on earthen site destruction. Furthermore, it should be beneficial for the heritage management to use four different core population models, providing a helpful theoretical basis for protection measures for earthen sites at a certain distance from the place where people gather, such as the addition of the fence and monitoring systems.

Specifically, by collecting the population number and region area of the village, a conservationist can calculate the theoretical damage degree of an earthen site located outside or inside of a village with the help of the single core population distribution model to determine the level of preventative effort, and definitely, the data of distance between the site and village are necessary to process this calculation.

Results and discussion

Linear absent section ratio (L-ASR)

The authors first calculated the L-ASR value of the No.1 of Chengbeihou Castle by measuring its size on the plane graph in Auto CAD. As shown in Fig. 3, with the side lengths of 123 and 86 m, the CL and RL are 418 and 149.4 m, respectively (the lengths of the east wall, south wall, west wall and north wall are 2.5, 62.1, 38.1, and 46.7 m). After that, on the basis of Eq. (1), its RLR and L-ASR are 35.74 and 64.26%. Other castle plane maps can be seen in the Additional file 1, except for No. 39 and No. 43 Castles (they are seriously damaged and their plan cannot be distinguished). The length data and L-ASR values for all 46 castles are listed in Table 3.

In Table 3, the conservation status of each castle can be acquired based on the L-ASR values and corresponding classification ranges: there are no castles with an excellent status; 10 castles have a good status, making up 22% of the total castles; 9 castles have a fair status, accounting for 20%; 10 castles (22%) have a poor status, and 16 castles (36%) have a very poor status (Fig. 4). Hence, castles with excellent status constituted the minimum proportion, while castles with very poor status represented the largest percentage. More than half of the castles are in poor condition or worse. These grading evaluation results reflect the grave situation of the earthen sites. Furthermore, the authors compared the conservation status of castles in G, F, P, and VP levels determined by the L-ASR index with their actual situation by choosing four representative castles (No. 18, 20, 40 and 45 castles), which can be seen in Fig. 4. According to this comparison, the castles were damaged more seriously as the damage level calculated by the indicator of L-ASR increased.

These research methods and results could provide helpful and effective suggestions for the conservation status of the 46 castles because the L-ASR is a very useful indicator to reflect the overall damage or material

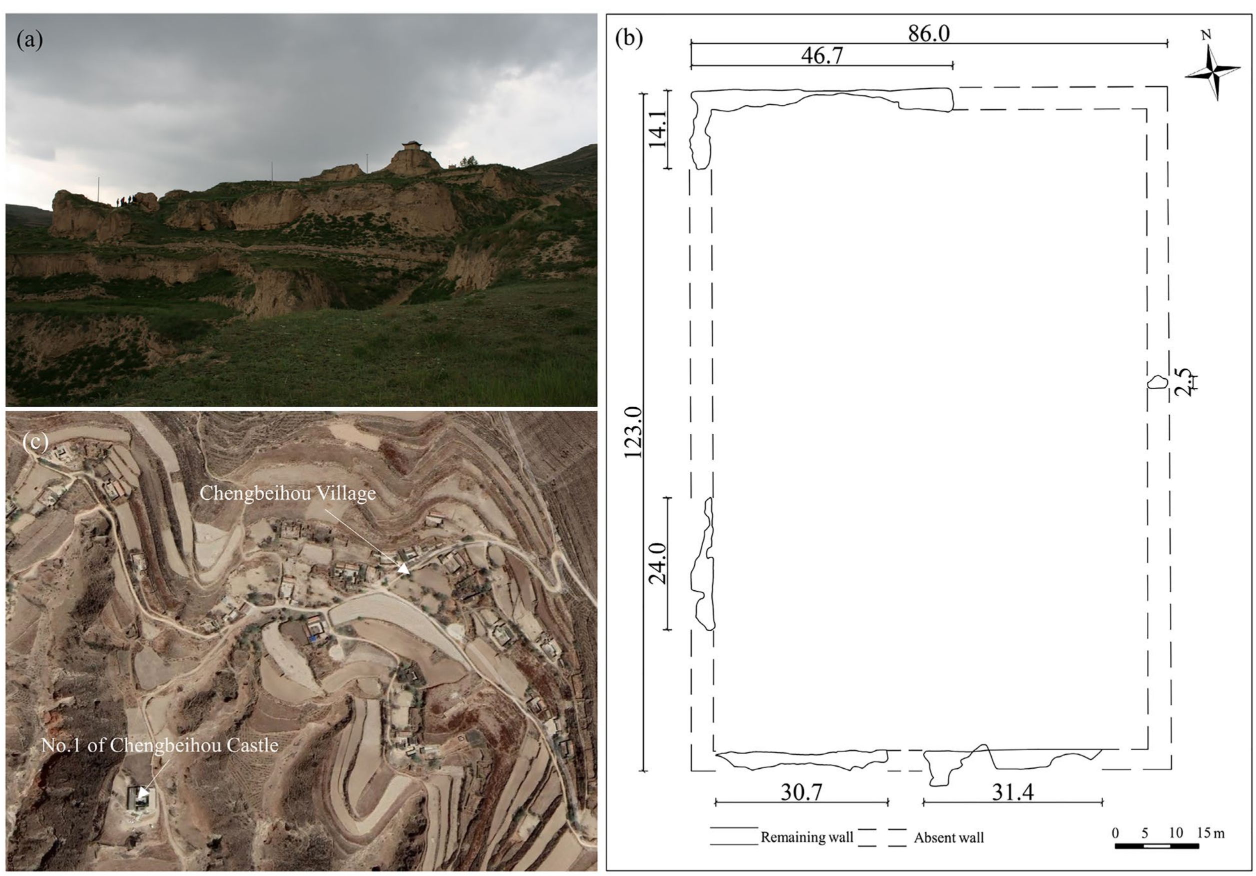

Fig. 3 No.1 of Chengbeihou Castle: **a** front view, **b** plane graph, and **c** satellite image (from Google map)

Table 3 The length data and L-ASR of castles of the Ming Great Wall in Qinghai Province

Castle number	Circumference length (CL)	Remaining length (RL)	Remaining length ratio (RLR)	Linear absent section ratio (L-ASR)	Conservation status
1	418.00	149.40	35.74%	64.26%	P
2	68.00	32.50	47.79%	52.21%	P
3	400.00	305.80	76.45%	23.55%	G
4	82.20	20.40	24.82%	75.18%	VP
5	59.20	0.00	0.00%	100.00%	VP
6	294.00	235.00	79.93%	20.07%	G
7	188.00	86.35	45.93%	54.07%	P
8	134.00	18.00	13.43%	86.57%	VP
9	108.00	69.90	64.72%	35.28%	F
10	180.00	22.30	12.39%	87.61%	VP
11	182.00	48.40	26.59%	73.41%	P
12	220.00	7.50	3.41%	96.59%	VP
13	240.00	34.90	14.54%	85.46%	VP
14	315.00	9.93	3.15%	96.85%	VP
15	1572.00	465.25	29.60%	70.40%	P
16	542.00	114.00	21.03%	78.97%	VP
17	287.20	241.60	84.12%	15.88%	G
18	267.00	235.10	88.05%	11.95%	G
19	340.00	245.50	72.21%	27.79%	F
20	658.00	361.50	54.94%	45.06%	F
21	297.00	247.10	83.20%	16.80%	G
22	243.00	185.40	76.30%	23.70%	G
23	245.00	81.80	33.39%	66.61%	P
24	465.00	380.70	81.87%	18.13%	G
25	799.00	396.50	49.62%	50.38%	P
26	228.00	77.50	33.99%	66.01%	P
27	724.00	157.80	21.80%	78.20%	VP
28	166.00	102.30	61.63%	38.37%	F
29	952.00	151.80	15.95%	84.05%	VP
30	80.00	3.10	3.88%	96.13%	VP
31	66.00	8.00	12.12%	87.88%	VP
32	104.00	89.30	85.87%	14.13%	G
33	446.00	229.00	51.35%	48.65%	F
34	355.00	250.40	70.54%	29.46%	F
35	752.00	659.20	87.66%	12.34%	G
36	148.00	109.20	73.78%	26.22%	F
37	324.00	232.60	71.79%	28.21%	F
38	1320.00	126.70	9.60%	90.40%	VP
39	1100.00	7.00	0.64%	99.36%	VP
40	1093.00	470.67	43.06%	56.94%	P
41	1006.00	572.50	56.91%	43.09%	F
42	744.00	280.00	37.63%	62.37%	P
43	/	22.00	/	/	/
44	744.00	53.30	7.16%	92.84%	VP
45	4500.00	296.70	6.59%	93.41%	VP
46	2040.00	1531.60	75.08%	24.92%	G

Table 3 (continued)

The circumference length data of No. 43 castle cannot be obtained because it has been damaged very severely and from historical documents, there were no related records about its size

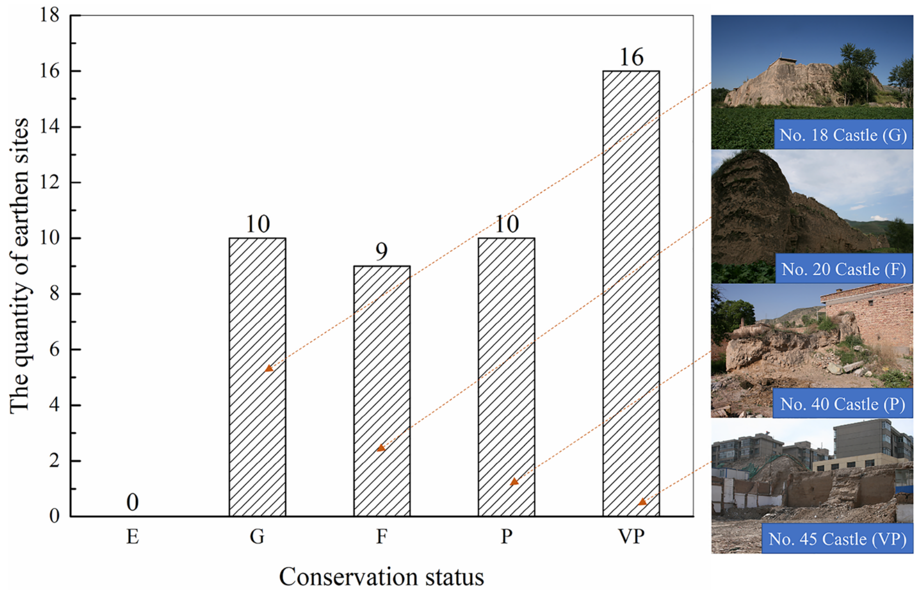

Fig. 4 The conservation status of castles in Qinghai Province

damage of the lineal cultural heritage sites since they were built up. Due to the extremely high artistic, scientific and social values of cultural heritages, it is of necessity to protect them, and prioritizing heritage conservation is a vital prerequisite for their subsequent protection. Therefore, prioritizing the site values during heritage conservation should be considered. However, quantifying the values of cultural heritage sites is still difficult because of their abstract properties. To address this issue, the authors introduced the administrative levels and military functions for castles in the military defense system of the Ming Great Wall (M-GWMDS), namely "Zhen, Lu, Wei, Suo, and Bao", from the highest to the lowest level [23], into the L-ASR results to further assess the site values and material losses. In the previous research, the specific level and military functions of the 46 castles in Qinghai Province have been clarified and can be divided into 7 types: Wei, Suo, courier station, the castle for garrison, Tusi's office or residence, horse keeping castles, and unofficial castles (last five types belong to Bao). Among them, the castle for garrison can be divided into two major categories, namely the garrison city and the garrison castle. Based on army types, the garrison castles have two classifications, i.e., cavalry camp and the garrison castle for defense [24, 25]. Combined with the L-ASR results, the relationship between the military functions and conservation status of castles in Qinghai Province can be obtained in Fig. 5. In general, when prioritizing castle conservation at the same level of conservation status based on L-ASR results, the value of castles should be taken into account so that a comprehensive consideration can be made, including the value levels and L-ASR results: the Wei castle should be given the highest values, as it is at the highest military level (the political, economic, and military center of M-GWMDS), Suo castles should have the secondary value level, and Bao castles should have the lowest level. In terms of the castle for garrison, the garrison city has a higher military level than the garrison castles based on the size of the architecture and the garrison, so it should have more values and higher priority ratings than the garrison castles.

Population density (PD)

In this study, most castles are located in or near a certain village. The authors collected the number of residential populations in these villages from archaeological materials provided by the Qinghai Bureau of Cultural Heritage, and measured the living area of such villages via Rivermap X3

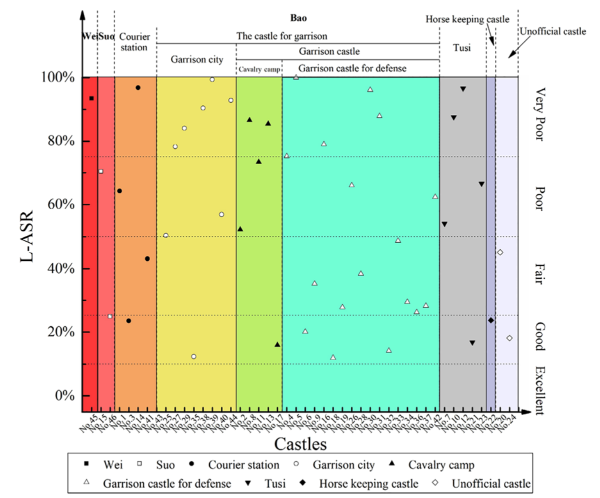

Fig. 5 The relationship between the military functions and conservation status of castles in Qinghai Province

software. Then the PD of the villages could be further calculated. The related data were listed in Table 4.

Combined with castle conservation status results previously acquired, the authors averaged all PD data of villages where the castles in each same damage level are located. As shown in the box plot (Fig. 6), with the increment of overall damage level, the average PD data steadily increased from 4860 per km^2 in the G status to 8679 per km^2 in the VP status. This means that the conservation status of earthen sites would worsen as the surrounding population grows from the perspective of data averaging.

The correlation between PD and L-ASR

After acquiring the PD data of villages and L-ASR of castles of the Ming Great Wall in Qinghai Province, the correlation between PD and L-ASR was studied to further reveal the anthropogenic influence on the conservation of earthen sites. In fact, many castles in this research are not located in villages but near those villages, so the population density attenuation along with the distance between castles and villages should be considered. Four frequently used single core population distribution models were applied, including the Clark, Smeed, Newling, and Cubic models [31–34], to calculate the population density of castles with the attenuation of the PD of villages that have a certain distance from castles.

The Clark model uses a negative exponential function to indicate the relationship between PD and distance from the residence center, as shown in Eq. (3):

$$PD_r = PD_0 e^{-br} \tag{3}$$

The Smeed model formula is a power exponential function shown in Eq. (4):

$$PD_r = PD_0 r^b \tag{4}$$

The Newling model is a quadratic exponential model shown in Eq. (5):

$$PD_r = PD_0 e^{br + cr^2} \tag{5}$$

The Cubic model is a cubic function from Eq. (6):

$$PD_r = PD_0 e^{br + cr^2 + dr^3} \tag{6}$$

where PD_r is the population density of a place with a distance of r from the residence center, PD_0 is the population density of the residence center, and b, c and d are parameters. In this study, if a castle was located in a village, then its distance was regarded as 0 m; if it was located outside of a village, then its distance was measured between the centers of the castle and the nearest village. The population distribution is assumed to be the single core, meaning that a single village's influence on castle damage was only considered. Furthermore, the PD_r is the assumed population density of castles with the attenuation of the PD of villages, PD_0 is the population density of villages, and r is the distance between the castle and village.

Combined with related archaeological materials and Rivermap X3 software, we collected and measured the data of distances between castles and villages in which they were located or nearby, as listed in Table 4. After that, it is assumed that there is a linear positive correlation between PD_r and L-ASR. During processing the related data, the PD_0 and L-ASR of castles that have the same distance from villages where they are located were calculated as the average value. Eventually, there were 17 groups of data to conduct the fitting, which are shown in Table 5.

To achieve optimal fitting effects, the Levenberg–Marquardt (LM) optimization algorithm was used to determine the parameters in Eqs. (3–6). After that, PD_r can be calculated and the correlation between PD_r and L-ASR can be further determined, as shown in Fig. 7. From the correlation results, the Cubic model has the largest correlation coefficient ($R = 0.6415$), compared to the other three models. Therefore, the positive correlation between PD and L-ASR can be proved, and the anthropogenic influence on the conservation of earthen sites was revealed from a macroscopic perspective. The 3D data (DEM) were applied to illustrate the conservation status of earthen sites, as shown in Fig. 8. The Cubic model has been used to show the anthropogenic influence from the PD perspective on the destruction of earthen sites by taking No. 1 and No. 2 castles as an

Table 4 The population density and distance of villages where the castles of the Ming Great Wall in Qinghai Province are located or nearby

Castle number	The name of the village	The number of population (PN)	The living area of the village (RA)/km^2	Population density (PD)/ number per km^2	The distance between castles and villages (r)/km
1	Chengbeihou Village	350	0.0532	6575	0.200
2	Chengbeihou Village	350	0.0532	6575	0.500
3	Najiazhuang Village	40	0.0044	8999	0.800
4	Mengjia Bay Village	500	0.0701	7129	/
5	/	/	/	/	/
6	Nianxiangou Village	80	0.0309	2588	0.126
7	Naozhuang Village	800	0.3494	2290	0.000
8	Simozhuang Village	700	0.0363	19,295	1.710
9	Simozhuang Village	700	0.0363	19,295	0.000
10	Shangyamen Village	1000	0.2127	4702	0.300
11	Lianxing Village	300	0.0507	5918	0.000
12	Qijiabao Village	1000	0.1146	8727	0.000
13	DieergouVillage	400	0.0518	7716	0.000
14	Laoya Village	2000	0.1590	12,579	0.130
15	Dengjia Village	2000	0.1644	12,168	0.170
16	Yuanjiazhuang Village	900	0.0799	11,271	0.200
17	Maying Village	200	0.0240	8331	0.280
18	Beizhuang Village	600	0.1272	4716	0.000
19	Shijia Village	1000	0.1255	7966	0.480
20	Xintianbao Village	700	0.2015	3474	0.000
21	Baiya Village	700	0.2609	2683	0.000
22	Datongyuan Village	2000	0.3099	6454	0.000
23	Chenjiatai Village	700	0.1236	5664	0.000
24	Xiamaquan No.2 Village	1000	0.2619	3819	0.038
25	Gucheng Village	1000	0.0580	17,250	0.226
26	Xiamiaogou Village	500	0.1102	4538	0.050
27	Xincheng Village	1386	0.1966	7049	0.000
28	Pingle Village	500	0.3005	1664	0.300
29	Gucheng Village	500	0.3180	1573	0.000
30	Yangpotai Village	795	0.0655	12,147	0.700
31	Shangxinzhuang Village	2534	0.6115	4144	0.000
32	Boshiying Village	1126	0.2607	4319	0.290
33	Eastern Village of Lushaer Town	2116	0.2989	7079	0.000
34	Jiaerzang Village	2070	0.7228	2864	0.000
35	Xincheng Village	1206	0.2734	4412	0.000
36	Yuanershan Village	2136	0.4322	4942	0.300
37	Dongjia Bay Village	1581	0.4102	3854	0.280
38	Xujiazhai Village	2109	0.4396	4798	0.000
39	Tonghai downtown Village	1903	0.5467	3481	0.000
40	Songshu Village	500	0.1311	3815	0.210
41	Gushan Village	2000	0.7129	2805	0.000
42	Baijia Village	1863	0.1191	15,641	0.000
43	Pingan Village in town	1300	0.2099	6194	0.000
44	Zongnan Village	2000	0.3065	6525	0.000
45	Urban district of Xining City	200,000	10.5000	19,048	0.000
46	Heyin Town	22,843	10.0100	2282	0.000

The No. 4 castle is far away from the village, and there is no village close to the No. 5 castle, so the distances between these castles and villages were not considered in this research

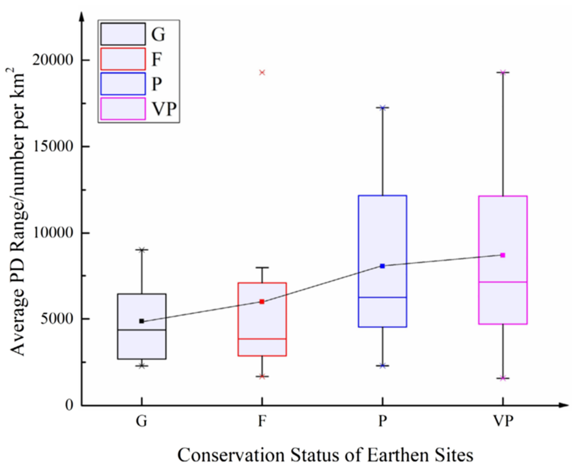

Fig. 6 Box plot illustrating the tendency between PD and conservation status of castles in Qinghai Province

example. Figure 8 shows the spatial distribution of the conservation status of castles and the PD distribution obtained by applying the Cubic model to the Chengbeihou Village, and its nearby castles, i.e., the No. 1 and No. 2 castles.

It is true that if more than one village was close to one certain castle, they would contribute to its damage. We surveyed all castles in this study and found that 24 castles were located in villages, 19 castles were located near villages within 1 km, and the others were far away from villages. For the castles near villages, we found that there was only 1 village in the distance range (1 km) of a certain castle, and villages with a distance greater than 1 km were not considered in the population distribution modeling. The reason is that the single core population distribution model can be a convenient and efficient tool to calculate the population density of castles with the attenuation of the PD of villages that have a certain distance from castles. If we consider villages more than 1 km from castles, the multicore population distribution model should be further researched and applied, which is a complex issue because more village population data are needed to process the fitting. However, population data in such far side villages are lacking. In fact, the population data were collected from the comprehensive investigations on the Great Wall from 2007 to 2009 organized by the Qinghai Provincial Administration of Cultural Relics and the Qinghai Bureau of Surveying and Mapping, and the team only collected the population data of the nearest villages from the castles. Therefore, it is difficult to consider the multicore population distribution model to study more villages contributing to the damage of castles. We acknowledge that there is a distance limitation in that our study only considered the influence of the nearest village on castle damage in the distance range of 1 km. In our future study, we will try to collect and expand more population data of villages in the application of the multicore population distribution model.

Table 5 The groups of fitting data in this research

Number of group	Average villages population density (PD_0)/number per km^2	Average distance between castles and villages (r)/km	Average linear absent Ratio (L-ASR)
1	6451	0.000	58.95%
2	3819	0.038	18.13%
3	4538	0.050	66.01%
4	2588	0.126	20.07%
5	12,579	0.130	96.85%
6	12,168	0.170	70.40%
7	8923	0.200	71.61%
8	3815	0.210	56.94%
9	17,250	0.226	50.38%
10	6093	0.280	22.04%
11	4319	0.290	14.13%
12	3769	0.300	50.73%
13	7966	0.480	27.79%
14	6575	0.500	52.21%
15	12,147	0.700	96.13%
16	8999	0.800	23.55%
17	19,295	1.710	86.57%

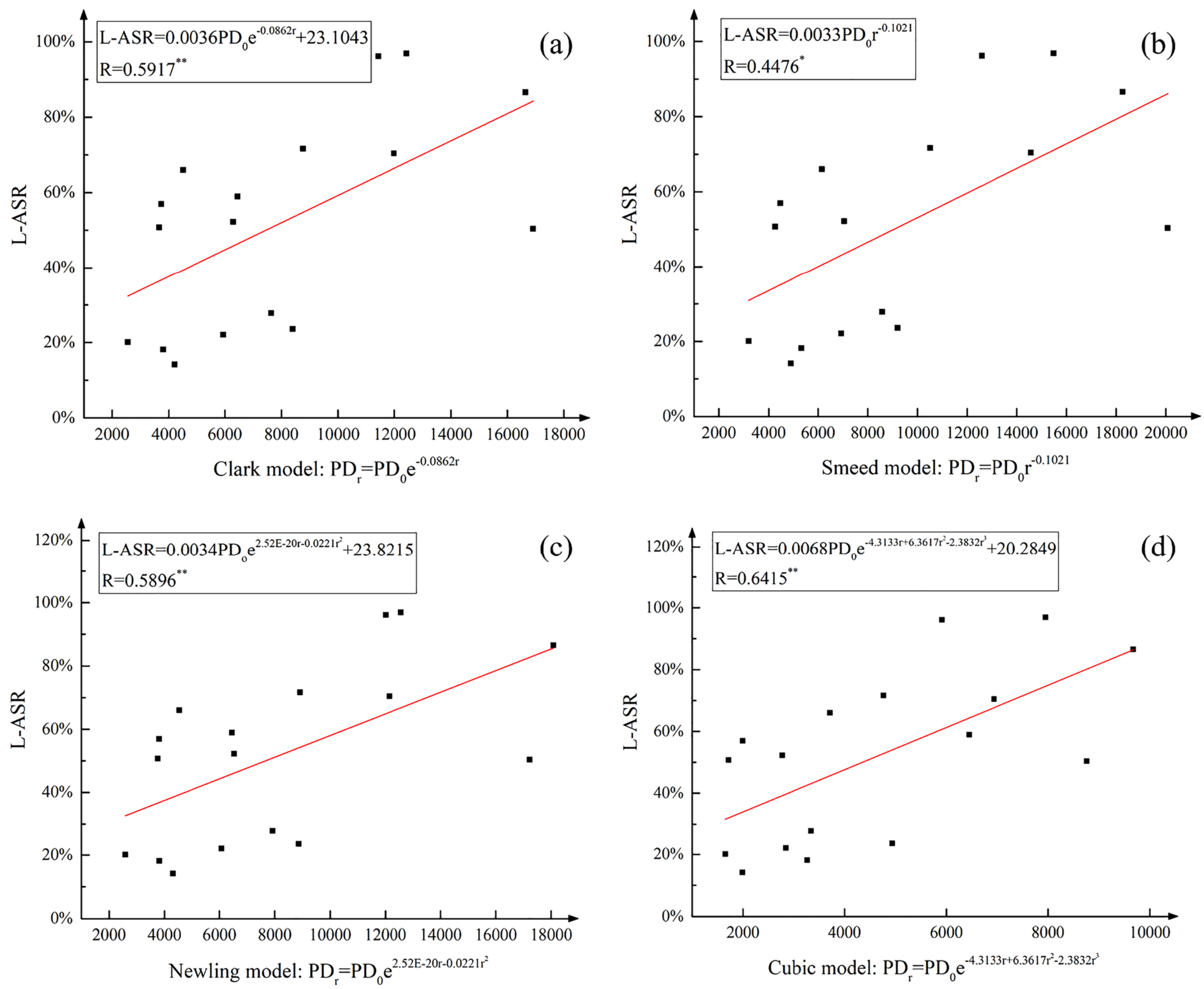

Fig. 7 The correlation graphs between PD_r and L-ASR: **a** Clark model, **b** Smeed model, **c** Newling model, and **d** Cubic model. * and ** represent the values of significance at 90% and 95% levels by the Student's t-test, respectively

In this research, there are benefits and limitations for the L-ASR indicator. One advantage is simplicity, because it can be briefly calculated from only two parameters, namely castle circumference length (CL) and remaining length (RL), to reflect the overall damage condition of earthen sites. Another advantage is the application of satellite imagery. The data of the living area of the village and the distance between castles and villages were collected from the satellite imagery via Rivermap X3 software. In our future research, the use of satellite imagery in earthen site conservation will be further explored. However, there is a limitation for the L-ASR indicator, which cannot reflect the conservation state of the remaining wall, i.e., there is no distinction if the remaining wall is in good/poor condition. In fact, this issue has been addressed in previous research. The vulnerability assessment has been studied by applying AHP-TOPSIS to determine the damage assessment levels for the remaining wall from 18 earthen sites in Qinghai Province, combined with their occurrence environment, engineering properties of rammed earth, deterioration characteristics, and building technologies [12]. Therefore, this research is actually a good supplement for the study on the damage assessment of earthen sites, as it has worked out the proportion of absent walls in the entirety of earthen sites, which was not given in that previous research. Another limitation is that we cannot obtain the related data to reflect the chronological moments of destruction of the properties in relation to their population. The population and architectural length data were

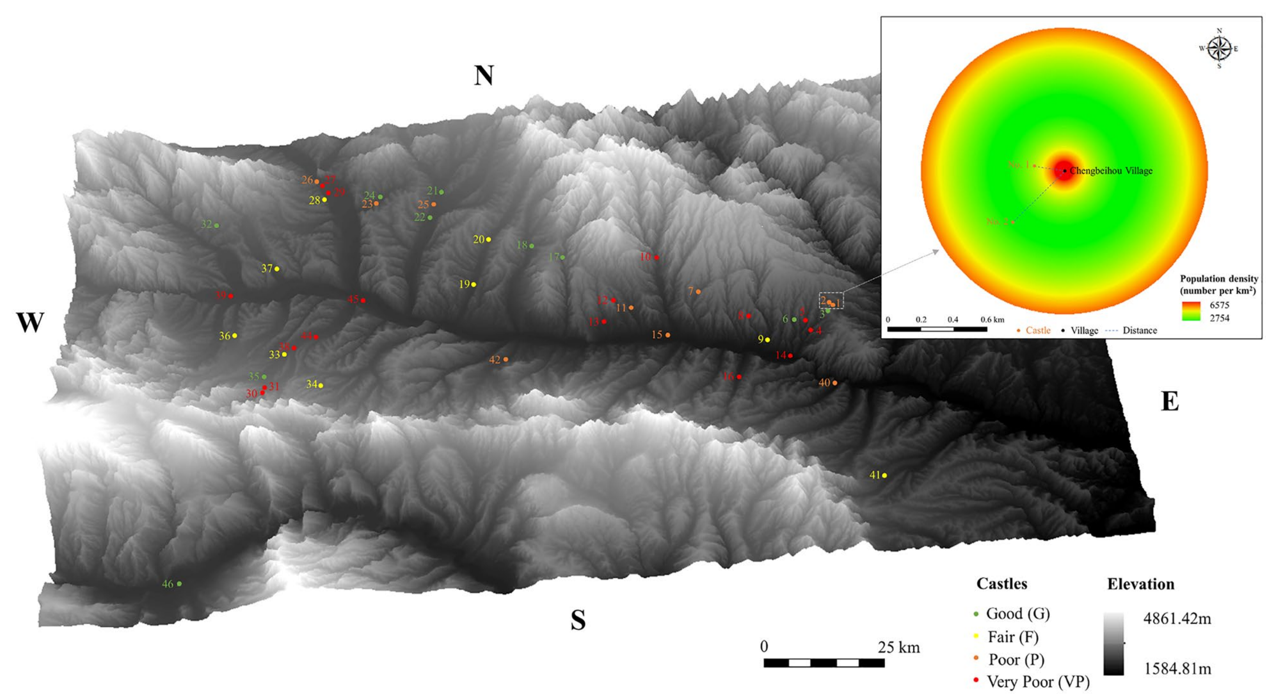

Fig. 8 Illustration of the conservation status of earthen sites

collected or calculated based on the archaeological materials in 2008 provided by the Qinghai Bureau of Cultural Heritage, which organized comprehensive investigations on the Ming Great Wall in Qinghai Province, China from 2007 to 2009. In fact, this is the only usable material to directly obtain the specific population of villages where castles were located either adjacent or nearby. The limitation is that these data can only reflect the population and destruction of castles in 2008. There are assumptions for this methodological proposal: The L-ASR index only considered the length of the plane of castles, while the height and volume of walls were not taken into account; The aforementioned four population distribution models have a common assumption with the single core population distribution, meaning that the population density would generally decrease with the increment of distance from the residential center. According to the average value of L-ASR for castles located in villages and castles outside of villages, we obtained that the average L-ASR for castles in villages is 58.95%, which is higher than the average L-ASR (54.27%) for castles outside villages. Based on the Cubic model in Eq. 6, the population density generally decreases with increasing distance from the residential center. Such results can jointly explain why heritage assets located in towns are more at risk of deterioration than those located in uninhabited environments. Therefore, if the castle is much closer to the village, its conservation could be more obviously affected by more intense human activities, which has been proved from the fitting correlation results in Fig. 7. The flaw is that the correlation coefficient is not very large. The reason is that the population number has fluctuated with time. In particular, the Ming Great Wall has been built for approximately 500 years but the residential number in their locations each year is difficult to acquire. However, a good corresponding relationship between PD and L-ASR was studied in this paper because they were both survey data organized in 2008; in addition to human influence, the damage to earthen sites is also closely related to the erosion of wind and rain and the vulnerability of rammed earth materials [12, 16]. To provide a far richer understanding of which factors correlate most strongly with deterioration, principal component analysis (PCA) was initialized using Minitab, including the population density calculated by the Cubic model, past climate data, and times of earthquakes per decade. The past climate data for the counties where 46 castles were located were collected from the Qinghai Meteorological Bureau, including annual rainfall and annual wind speed from 1961 to 2013, and the times of earthquakes per decade (2011–2021) were collected from the Data Sharing Infrastructure of National Earthquake Data Center [35], as listed in Table 6. The PCA results are shown in Table 7. The first three principal components accounted for 94.2% of the total variance, and rain and wind were the most relevant variables in the first principal component, while

Table 6 The factors data in the PCA research

Castle number	Counties	PD_r (number per km^2)	Annual rain (mm)	Annual wind speed (m/s)	Number of earthquakes per decade
1	Ledu	3513	298	1.84	722
2	Ledu	2778	298	1.84	722
3	Ledu	4974	298	1.84	722
4	Ledu	/	298	1.84	722
5	Ledu	/	298	1.84	722
6	Ledu	1655	298	1.84	722
7	Ledu	2290	298	1.84	722
8	Ledu	9965	298	1.84	722
9	Ledu	19,295	298	1.84	722
10	Ledu	2145	298	1.84	722
11	Ledu	5918	298	1.84	722
12	Ledu	8727	298	1.84	722
13	Ledu	7716	298	1.84	722
14	Ledu	7955	298	1.84	722
15	Ledu	6945	298	1.84	722
16	Ledu	6022	298	1.84	722
17	Huzhu	3894	600	1.29	451
18	Huzhu	4716	600	1.29	451
19	Huzhu	3351	600	1.29	451
20	Huzhu	3474	600	1.29	451
21	Huzhu	2683	600	1.29	451
22	Huzhu	6454	600	1.29	451
23	Huzhu	5664	600	1.29	451
24	Huzhu	3271	600	1.29	451
25	Huzhu	8766	600	1.29	451
26	Datong	3715	520	1.67	184
27	Datong	7049	520	1.67	184
28	Datong	759	520	1.67	184
29	Datong	1573	520	1.67	184
30	Datong	5945	334	1.61	395
31	Datong	4144	334	1.61	395
32	Datong	1994	334	1.61	395
33	Datong	7079	334	1.61	395
34	Datong	2864	334	1.61	395
35	Datong	4412	334	1.61	395
36	Datong	2254	334	1.61	395
37	Datong	1801	334	1.61	395
38	Datong	4798	334	1.61	395
39	Datong	3481	334	1.61	395
40	Minhe	1998	347	1.63	144
41	Minhe	2805	347	1.63	144
42	Pingan	15,641	335	2.29	380
43	Pingan	6194	335	2.29	380
44	Xining	6525	385	1.55	22
45	Xining	19,048	385	1.55	22
46	Guide	2282	368	1.95	102

Table 7 The PCA results

Eigenanalysis of the Correlation Matrix				
Eigenvalue	**2.0387**	**0.9497**	**0.7781**	**0.2335**
Proportion	0.510	0.237	0.195	0.058
Cumulative	0.510	0.747	0.942	1.000
Eigenvectors				
Variable	PC1	PC2	PC3	PC4
Population density	0.259	− 0.906	− 0.326	− 0.078
Annual rain	− 0.627	− 0.139	− 0.281	0.713
Annual wind speed	0.617	− 0.020	0.381	0.688
Number of Earthquakes	0.399	0.400	− 0.818	0.107

population density was the most relevant variable in the second principal component. For the third principal component, earthquakes were the most relevant variable.

A positive tendency between PD and L-ASR can be apparently seen from our research results, and the correlation coefficients passed the significance test and were statistically significant. Therefore, the indicator and model proposed in this research have scientificity and accuracy. In our future research, the L-ASR and PD models will be further promoted and applied to other sections of the Ming Great Wall in NW China to acquire more scientific and precise assessment outcomes of the conservation status of earthen sites by constantly revising and improving related parameters. Moreover, the volume reflection data including the remaining height and the top and bottom widths of earthen sites, will be collected, and then the volume absent section ratio (V-ASR) can be further studied in the future.

Conclusion

In this paper, 46 castles of the Ming Great Wall in Qinghai Province were chosen as research objects. The linear absent section ratio (L-ASR) was proposed to characterize the conservation status of earthen sites, which can be divided into five levels: excellent (E) (0–10%), good (G) (10–25%), fair (F) (25–50%), poor (P) (50–75%), and very poor (VP) (75–100%). By means of plane graphs of these castles, the remaining length (RL) and circumference length (CL) of castles were collected, and then L-ASR data were acquired.

Based on L-ASR values and corresponding classification ranges, there are no castles (0%) at the E status, 10 castles at the G status making up 22% of the total castles, 9 castles at the F status accounting for 20%, 10 castles (22%) at the P status, and 16 castles (36%) at the VP status, respectively. Hence, castles with excellent status constituted the minimum proportion (0%), while castles with very poor status represented the largest percentage (36%). More than half of the castles (58%) were in poor condition or even worse. These grading evaluation results reflect the grave situation of earthen sites.

Moreover, the population density (PD) of villages in which castles are located or nearby was obtained. Combined with the conservation status results of castles, the average PD data increased with the increment of overall damage level, meaning that the conservation status of earthen sites would worsen as the surrounding population grows from the perspective of data averaging.

By referring to four frequently used single core population distribution models, namely Clark, Smeed, Newling, and Cubic models, a linear positive correlation between the population density of a position where the castle is located (PD_r) and L-ASR was determined, and the Cubic model had the best fitting result. The population distribution model was the carrier to introduce an important factor in the quantitative study of the anthropologic influence on earthen site destruction, namely the distance between sites and villages. Furthermore, this is helpful for the heritage management by calculating the theoretical damage degree of an earthen site located outside or inside of a village. There are also main limitations in this research: the multicore population distribution model was not considered, and the chronological moments of destruction of the properties in relation to their population were not reflected due to the restrictions on receiving archaeological materials.

According to our research findings, the novel indicator, i.e., the L-ASR, can quantitatively characterize the ratio of an absent wall's linear length to the circumference length of castles by measuring the length of circumference length and remaining length, which is a very useful indicator to reflect the overall damage or material damage of the lineal cultural heritages since they were built up, and the anthropogenic influence on the damage of earthen sites has been revealed from a macroscopic perspective. This has the potential to further incorporate the indicator and model proposed in this research for the analysis of more various types of architecture with different materials or construction techniques, not only limited earthen sites, because the materials and techniques of buildings were not considered in the assessment process proposed in this research. As the L-ASR index only considered the length of the plane of castles, while the height and volume of the wall were not taken into account, the volumetric erosion of materials cannot be reflected at this moment. However, in our future research, the volume reflection data, including the remaining height and the top and bottom width of earthen sites will be collected, and then the volume absent section ratio (V-ASR) will be further studied. Therefore, this research is beneficial to the overall conservation assessment of earthen sites, and also meaningful to their further preservation and protective planning.

Abbreviations

L-ASR: Linear absent section ratio; PD: Population density; MDCM: Multicriteria decision-making; CL: Circumference length; RL: Remaining length; RLR: Remaining length ratio; E: Excellent; G: Good; F: Fair; P: Poor; VP: Very poor; RQD: Rock quality designation; PN: Population number; RA: Region area; M-GWMDS: Military defense system of the Ming Great Wall; V-ASR: Volume absent section ratio; PCA: Principal Component Analysis.

Supplementary Information

The online version contains supplementary material available at https://doi.org/10.1186/s40494-021-00582-5.

Additional file 1. Castles Plane Maps

Acknowledgements

This work was supported by the funding from the National Key R&D Plan Program of China (Grant No. 2020YFC1522201 and No. 2020YFC1521904), the cultural relics protection technology project of the State Administration of Cultural Heritage of the People's Republic of China (Grant No. 2013-YB-SQ-120), the National Natural Science Foundation of China (Grant No. 41562015 and No. 52068050), and the Fundamental Research Funds for the Chinese Central Universities (No. D5000210673). Acknowledgment for the data support from "China Earthquake Networks Center, National Earthquake Data Center. (http://data.earthquake.cn)", and help from Dr. Zhuo Chen in Sichuan Agricultural University.

Authors' contributions

YD and WC developed the methodology for this research. KC and WD were responsible for collecting the population and sites data. SZ and QZ were responsible for the model calculation. This manuscript was written by YD. YD also contributed to data analysis and processing. All authors read and approved the final manuscript.

Funding

This work was supported by the funding from the National Key R&D Plan Program of China (Grant No. 2020YFC1522201 and No. 2020YFC1521904), the cultural relics protection technology project of the State Administration of Cultural Heritage of the People's Republic of China (Grant No. 2013-YB-SQ-120), the National Natural Science Foundation of China (Grant No. 41562015 and No. 52068050), and the Fundamental Research Funds for the Chinese Central Universities (No. D5000210673).

Availability of data and materials

The data that support the findings of this study are available from the corresponding author upon reasonable request.

Declarations

Competing interests

The authors declare that they have no competing interests.

Author details

[1] Institute of Culture and Heritage, Northwestern Polytechnical University, Xi'an 710072, China. [2] Key Scientific Research Base of the State Administration of Cultural Heritage for the Conservation and Restoration of Murals and Material Science Research, Northwestern Polytechnical University, Xi'an 710072, China. [3] Key Laboratory of Mechanics on Disaster and Environment in Western China, College of Civil Engineering and Mechanics, Lanzhou University, 730000 Lanzhou, China. [4] Western Center for Disaster Mitigation in Civil Engineering of Ministry of Education of China, School of Civil Engineering, Lanzhou University of Technology, Lanzhou 730050, China.

Received: 13 May 2021 Accepted: 25 August 2021
Published online: 03 September 2021

References

1. Fujii Y, Fodde E, Watanabe K, Murakami K. Digital photogrammetry for the documentation of structural damage in earthen archaeological sites: the case of Ajina Tepa. Tajikistan Eng Geol. 2009;105:124–33.
2. Elert K, Sebastián E, Valverde I, Rodriguez-Navarro C. Alkaline treatment of clay minerals from the Alhambra Formation: implications for the conservation of earthen architecture. Appl Clay Sci. 2008;39:122–32.
3. Matero F. Lessons from the Great House: Condition and treatment history as prologue to site conservation and management at Casa Grande Ruins National Monument. Conserv Manag Archaeol Sites. 1999;3:205–24.
4. Lercari N. Monitoring earthen archaeological heritage using multi-temporal terrestrial laser scanning and surface change detection. J Cult Herit. 2019;39:152–65.
5. Du Y, Chen W, Cui K, Gong S, Pu T, Fu X. A model characterizing deterioration at earthen sites of the Ming Great Wall in Qinghai Province. China Soil Mech Found Eng. 2017;53:426–34.
6. Luo Y, Yang M, Ni P, Peng X, Yuan X. Degradation of rammed earth under wind-driven rain: the case of Fujian Tulou. China Constr Build Mater. 2020;261:119989.
7. Jaquin PA, Augarde CE, Gerrard CM. Chronological description of the spatial development of rammed earth techniques. Int J Archit Herit. 2008;2:377–400.
8. Blanco-Rotea R, Costa-García JM, Fonte J, Gago M, Gonçalves JA. A Modern Age redoubt in a possible Roman camp. The relationship between two defensive models in Campos (Vila Nova de Cerveira, Minho Valley, Portugal). J Archaeol Sci Rep. 2016;10:293–308.
9. Costa C, Cerqueira Â, Rocha F, Velosa A. The sustainability of adobe construction: past to future. Int J Archit Herit. 2019;13:639–47.
10. Pei QQ, Wang XD, Zhao LY, Zhang B, Guo QL. A sticky rice paste preparation method for reinforcing earthen heritage sites. J Cult Herit. 2020;44:98–109.
11. Wang X, Li Z, Chen W, Zhang H, Guo Q, Sun M, Wang S, Zhang B. Research on key technologies for the protection of earth sites. Beijing: Science Press; 2013.
12. Du Y, Chen W, Cui K, Zhang K. Study on damage assessment of earthen sites of the Ming Great Wall in Qinghai Province based on Fuzzy-AHP and AHP-TOPSIS. Int J Archit Herit. 2020;14:903–16.
13. Li L, Shao M, Wang S, Li Z. Preservation of earthen heritage sites on the Silk Road, northwest China from the impact of the environment. Environ Earth Sci. 2011;64:1625–39.
14. Richards J, Zhao G, Zhang H, Viles H. A controlled field experiment to investigate the deterioration of earthen heritage by wind and rain. Herit Sci. 2019;7:1–13.
15. Shao M, Li L, Wang S, Wang E, Li Z. Deterioration mechanisms of building materials of Jiaohe ruins in China. J Cult Herit. 2013;14:38–44.
16. Du Y, Chen W, Cui K, Zhang J, Chen Z, Zhang Q. Damage assessment of earthen sites of the Ming Great Wall in Qinghai Province: a comparison between Support Vector Machine (SVM) and BP Neural Network. J Comput Cult Herit. 2020;13:1–18.
17. Porter DW, Mehrotra A, DeJong MJ, Bass A, Guebard M, Ochsendorf J. Material and seismic assessment of the Great House at Casa Grande Ruins National Monument. Arizona J Archit Eng. 2020;26:05019007.
18. Richards J, Viles H, Guo Q. The importance of wind as a driver of earthen heritage deterioration in dryland environments. Geomorphology. 2020;369:107363.
19. Wu Z, Wei Y. The widespread consultation of the overall protective planning of the Ming Great Wall in Qinghai Province. Gt Wall 2016;2016:53–4.
20. Xu Y, Xu X, Tang Q. Human activity intensity of land surface: Concept, methods and application in China. J Geogr Sci. 2016;26:1349–61.
21. Su MM, Wall G. Community participation in tourism at a World Heritage Site: Mutianyu Great Wall, Beijing. China Int J Tour Res. 2014;16:146–56.
22. Chen W, Du Y, Cui K, Fu X, Gong S. Architectural forms and distribution characteristics of beacon towers of the Ming Great Wall in Qinghai Province. J Asian Archit Build Eng. 2017;16:503–10.

23. Cao Y, Zhang Y. The fractal structure of the Ming Great Wall Military Defense System: a revised horizon over the relationship between the Great Wall and the military defense settlements. J Cult Herit. 2018;33:159–69.
24. Du Y, Chen W, Cui K, Guo Z, Wu G, Ren X. An exploration of the military defense system of the Ming Great Wall in Qinghai Province from the perspective of castle-based military settlements. Archaeol Anthropol Sci. 2021;13:46.
25. Ren X. Resources' investigation report of Ming Great Wall in Qinghai Province. Beijing: Cultural Relics Press; 2012.
26. Pu T, Chen W, Du Y, Li W, Su N. Snowfall-related deterioration behavior of the Ming Great Wall in the eastern Qinghai-Tibet Plateau. Nat Hazards. 2016;84:1539–50.
27. Xie D, Zhao X, Pang Y. A study on spatial distribution and hierarchy of Chinese Jin Great Wall defensive settlements. In: 2015 international conference on industrial technology and management science (ITMS 2015); 2015.
28. Chen J, Jin S, Liao A, Zhao Y, Zhang H, Rong D, Yang Z. Stereo mapping of Ming Great Wall with remote sensing. Chin Sci Bull. 2010;55:2290–4.
29. Deere DU. Deere DW (1988) The rock quality designation (RQD) index in practice. In: Kirkaldie L, editor. ASTM-STP 984. Philadelphia: American Society for Testing and Materials; 1988. p. 91–101.
30. Smailes PJ, Argent N, Griffin TLC. Rural population density: its impact on social and demographic aspects of rural communities. J Rural Stud. 2002;18:385–404.
31. Clark C. Urban population densities. J R Stat Soc Ser A. 1951;114:490–6.
32. Smeed RJ. The effect of some kinds of routeing systems on the amount of traffic in the central areas of towns. J Inst Highw Eng. 1963;10:5–26.
33. Newling BE. The spatial variation of urban population densities. Geogr Rev. 1969;59:242–52.
34. Frankena MW. A bias in estimating urban population density functions. J Urban Econ. 1978;5:35–45.
35. Data Sharing Infrastructure of National Earthquake Data Center. http://data.earthquake.cn.

Publisher's Note